Experimental Methods and Magnetic Materials

E. Burzo

Faculty of Physics, Babes-Bolyai University Cluj-Napoca, Romania

The understanding of complex magnetic behaviour of magnetic materials was strongly related to development of new experimental methods. The experimental evidence was followed, in many cases, by the elaboration of theoretical models devoted to understanding their physical basis. The earlier studies were focused in analyzing the temperature and field dependences of magnetization and magnetic susceptibility. Weiss [1] developed the molecular field approximation in order to describe the experimental evidence. The postulates concerning the existence of magnetic domains and the presence of molecular field, H_m=NM, proportional to magnetization constituted the basis for understanding the physical properties of simple magnetic systems. Latter on, by development of experimental methods, evidence of magnetic domains was found (Barkhausen effect, Kerr effect). The band models were also developed in order to explain the magnetic behavior of ferromagnetic metals and alloys. The molecular field coefficient N was related to exchange integral.

The elaboration of new types materials, as for example ferrites of garnets, evidenced rather complicated evolution with temperature of magnetization and magnetic susceptibility. Although at this time no evidence for the orientation of magnetic moments at various sites, was possible, Néel [2] elaborated the model of ferrimagnetism which explained the $M_s$vsT and χvsT dependences. The development of neutron diffraction method confirmed the assumptions of the orientation of magnetic moments proposed by Néel. The neutron diffraction method is now widely used to study the magnetic materials. In Fig.1 we present the thermal variations of magnetizations and reciprocal susceptibilities for ferrimagnetic RFe_2(R=Dy,Ho,Er,Tm) compounds, which crystallize in a cubic type structure [3]. The neutron diffraction studies – Fig.2 [4] showed that the rare-earth and iron moments are antiparallely oriented. Analyzing the thermal variations of magnetization can be seen that there is a compensation point of the two sublattices magnetizations in $ErFe_2$, but such compensation cannot be evidenced in $HoFe_2$, confirming the results of magnetic measurements. This method allowed to analyze complex magnetic structures or to obtain the magnetization density. As example in Fig.3a we plotted the magnetic structures and the magnetic moments as function of temperature as well as the angle φ between the direction of magnetic moments and **c**-axis for a ferromagnetic $NdCo_5$ and ferrimagnetic $TbCo_5$ compound [5]. The magnetizations in field of $\mu_0 H \cong 2T$ are also plotted. The magnetic moments orientations change from perpendicular to **c**-axis to parallel to **c**-axis as temperature increases. There is a noncoleniarity of the magnetic structure during the reorientation process [6] – Fig.4. In ferromagnetic compounds, the direction of resultant magnetization M_s is close to those of M_{Co} and M_R and thus the evidence for noncoleniarity of the magnetic structure is very difficult to be obtained experimentally. A more favorable situation is obtained in the ferrimagnetic compounds.

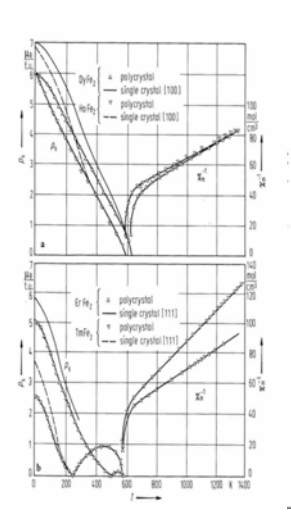

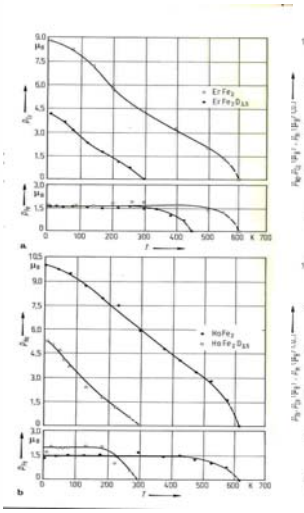

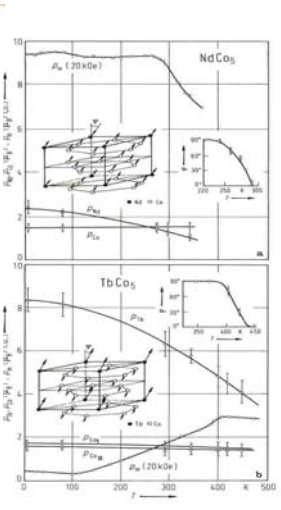

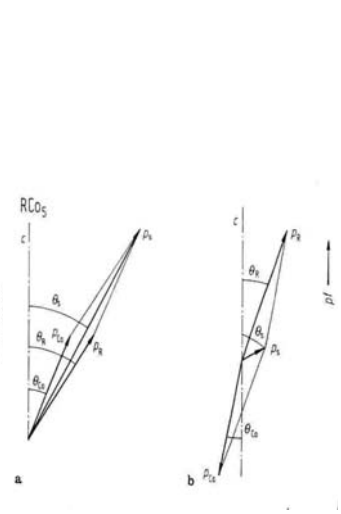

Fig.1 Fig.2 Fig.3 Fig.4

The development of electron paramagnetic resonance (EPR) [7] and ferromagnetic resonance (FMR) [8] methods contributed further to the understanding the magnetic phenomena. The spin and orbital contributions were determined. For example, by FMR, values of the spectroscopic splitting factors for Fe (g=2.05-2.09), Co (g=2.18-2.23) and Ni (g=2.17-2.22) were reported. The studies were extended on ferromagnetic intermetallic compounds – Fig.5a [9]. In case of $Y(Fe_xAl_{1-x})_2$ a value g=2.07(1) was obtained, independent on composition. For $Y(Fe_xCo_{1-x})_2$ compounds, were both Fe and Co are magnetic, the g values were described by the relation $g = (M_{Fe} + M_{Co})(M_{Fe}g_{Fe}^{-1} + M_{Co}g_{Co}^{-1})^{-1}$. The spectroscopic splitting factors g_{Fe}=2.08(1) and g_{Co}=2.18(2), were determined by using the values of sublattices magnetizations M_{Fe} and M_{Co} deduced from magnetic and Mössbauer effect measurements. In case of ferrimagnetic compounds, as for example $(Gd_xY_{1-x})Fe_2$, by magnetic resonance only an effective g factor can be obtained, as expressed by the Vangsness relation [10]: $g_{eff} = (M_{Gd} - M_{Fe})(M_{Gd}g_{Gd}^{-1} - M_{Fe}g_{Fe}^{-1})^{-1}$. By using the M_{Gd} and M_{Fe} sublattice magnetizations and fitting the experimental data according to above relation – Fig.5b – values g_{Gd}=2.00 and g_{Fe}=2.10(2) were obtained [11]. The above data show that the g values of the transition metals are not sensitively modified by alloying. The dynamical equations (Landau-Lifshitz, Gilbert, Bloch-Bloembergen, Callen) [12] allowed not only to analyze the resonance phenomena but now are used in describing the magnetization processes of the nanomaterials.

The electron paramagnetic resonance method was used to study magnetic properties of various systems, particularly the exchange integral, by considering an RKKY model. The exchange integral, in this model, in proportional to the shift of g value as compared to that characteristic in a diamagnetic matrix. The analysis of the data is complicated by the presence of bottleneck effects. The concentration dependences of the g shift and Korringa broadening in $Gd_xY_{1-x}Cu$ system are given in Fig. 6 [13]. A positive g-shift and a drastic increase of the Korringa slope were shown for x<<1. For a high Gd content there are bottleneck effects. For samples with x<<1, the bottleneck is open and a real value of the exchange integral can be obtained. The role of s- and d- conduction electrons to the exchange interactions can be thus analysed.

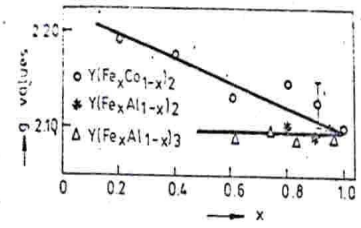

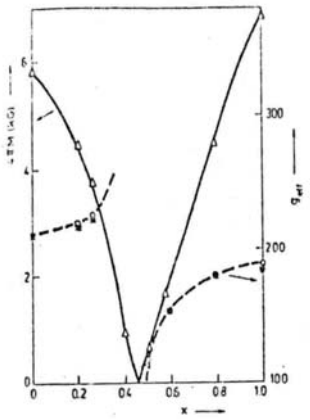

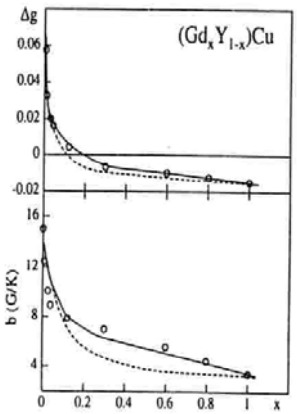

Fig.5a Fig.5b Fig.6

The nuclear resonance method (RMN) was elaborated in 1946 [14]. By this method is analysed the nuclear spin in an uniform magnetic field, on the sample acting a radio frequency field. For magnetic ordered materials, the resonance can be obtained only in internal field. For example, in Fig.7a we plotted the NMR spin echo spectra at the Y sites in $Y(Fe_{1-x}Co_x)_2$ ($0 \leq x 0.8$) compounds, at 4.2 K, in zero external magnetic field [15]. Starting from the line at 46 MHz in pure YFe_2 (representing the situation with 12 Fe neighbours atoms) and counting out the satellites, the different (Fe,Co) configurations have been assigned to these satellites as indicated. In the Fig.7b the spin-echo spectra of ^{59}Co in $Y(Fe_{1-x}Co_x)_2$, at 77K, in zero external magnetic fields are plotted [16]. The substitution of Co by Fe gives rise to a developed satellite structure in the low Co concentration range. For high Co content there are superposition of resonance lines from various nearest neighbour configurations and only their envelope was obtained. The mean values of the hyperfine fields decrease as Fe is replaced by Co. These data show the effects of local environments on the magnetic properties.

Mössbauer effect is an useful tool to investigate the magnetic behaviour of the probe nuclei in a solid [17]. The isomer shift is the result of electrostatic interaction between the charge distribution in the nucleus and s electrons, quadrupole splitting gives information on the symmetry of probe nucleus and hyperfine fields on their magnetic behaviour. The ^{57}Fe Mössbauer spectra in $DyFe_2$, $DyFe_2H_{1.92}$ and ^{161}Dy in $DyFe_2H_{1.92}$ are plotted in Fig.8 [18]. In $DyFe_2$ only one ^{57}Fe magnetic hyperfine field spectrum was observed corresponding to a single crystallographic and magnetic site $(\bar{3}m)$. The spectrum for hydride is more complex and shows resolved structure in spite of slightly broader resonance as compared to $DyFe_2$ and was analysed as a superposition of two six lines magnetic hyperfine spectra.

The different types of Fe sites in hydride were associated with differences in the number and/or positions of surrounding hydrogen atoms. The two distinct sites suggest that the hydrogen forms an ordered structure at this composition. The ^{161}Dy spectrum of $DyFe_2H_{1.92}$, at 4.2 K, shows the presence of a single hyperfine field of 6050(50) kOe, which is close to the free ion value (6200 kOe) but less than the value of 7080 kOe for $DyFe_2$. Hence the saturated Dy magnetic moment in hydride, although somewhat reduced from the enhanced magnetic moment in $DyFe_2$ (due to 5d band polarization), is still close to the free ion value of 10 μ_B. We note that in the first approximation, the ^{57}Fe hyperfine field is proportional to iron magnetic moment – Fig. 9 [11].

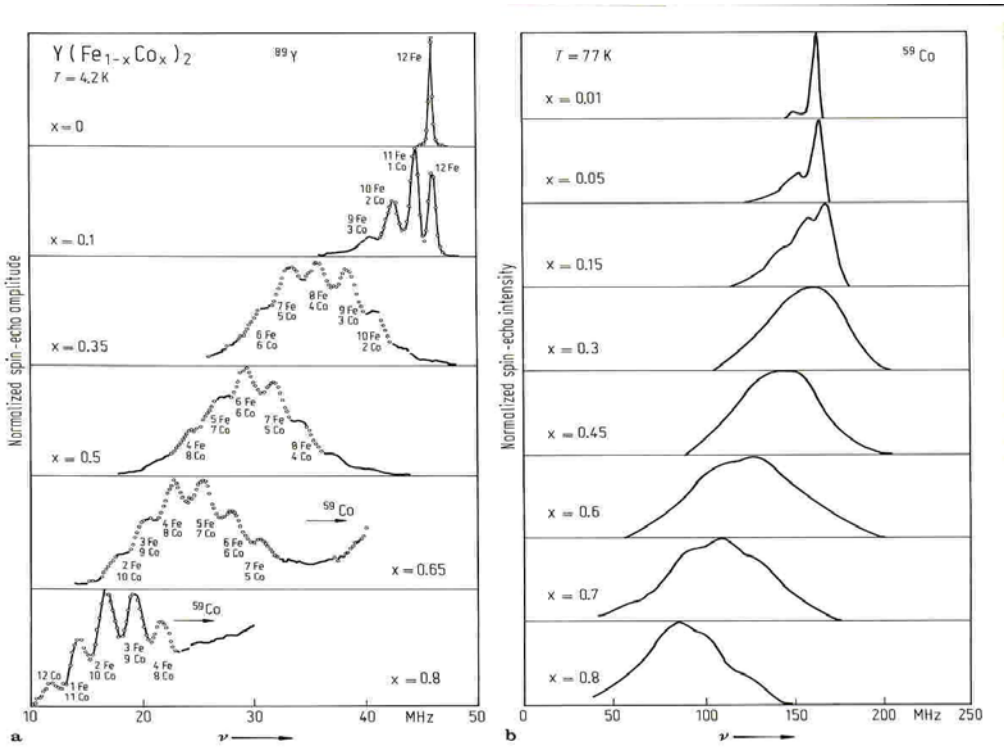

Fig. 7

For complex compositions as that of natural diopside (ideal $Ca(Mg,Fe)Si_2O_6$), where substitutions at Ca (M2 site), Mg (M1 site) and Si site are present, both Fe^{2+} and Fe^{3+} ions were found [19]. Both ^{57}Fe spectra exhibit broad quadrupole-splitting distributions (QSD), indicating widely fluctuating chemical and structural environments for the probe Fe nuclei. The numerical analysis based upon a shape independent distribution fitting, using superposition of the ferrous and ferric QSD with single, but different isomer shifts for each of the two iron valence states were found to describe adequate the experimental line shapes – Fig.10. The two maxima in the ferric $P(\Delta Q)$ distributions might indicate the presence of Fe^{3+} in two different M1 sites, related to the Al- for Si substitution and that additional broadening of the individual components results from different cation configurations in the next-nearest neighbour shells.

The X-ray photoelectron spectroscopy (XPS) studies may suply useful information on the magnetic behaviour. Two examples will be mentioned, concerning $LaNi_5$-band systems and Mn-perovskites. $LaNi_5$ was considered long time as a normal paramagnet. The careful analysis of the magnetic properties shows a transition from a T^2 dependence of the magnetic susceptibilities, at $T \leq 10$ K, to a Curie-Weiss behaviour at $T > T^* \cong 200$ K – Fig.11a. An effective nickel moments of 2.15 μ_B/atom was determined. The XPS valence band of $LaNi_5$, at RT, shows a similarity to that of Ni3d band in pure nickel – Fig.11b [20]. This fact evidences that the valence band of $LaNi_5$ is mainly derived from Ni3d band. In addition, as in pure Ni, there is a structure at about 6eV binding energy, which suggests the presence of holes in Ni3d band.

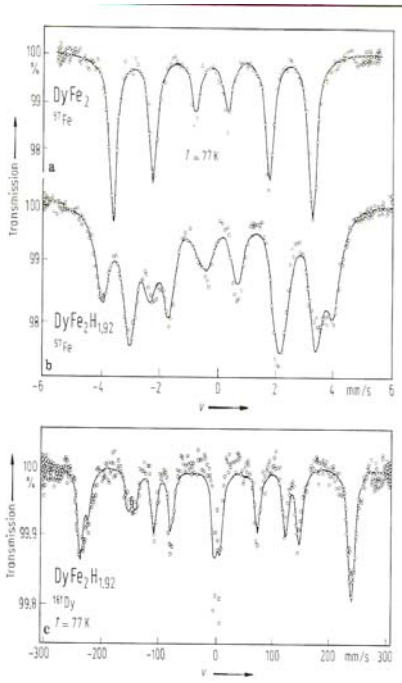

Fig.8

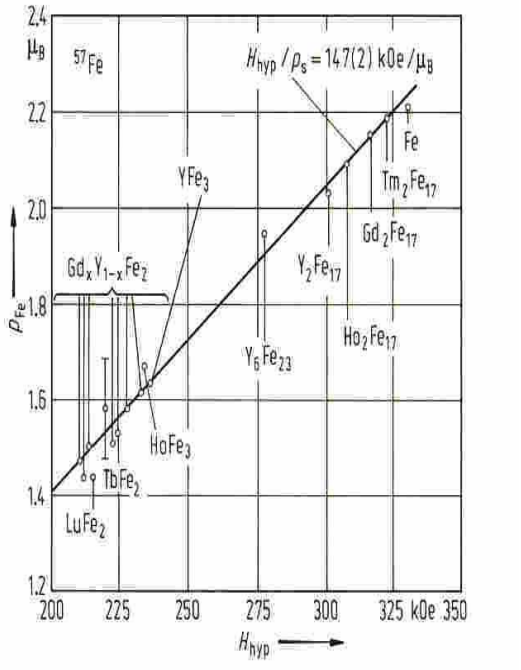

Fig.9

Mn3s XPS spectrum consists of two spectral lines that are belived to be due to exchange interactions of Mn3s and 3d electrons. These reflect the energy difference between photoemission final states with 3d spin parallel or antiparallel. The exchange interactions are dependent on the valence state of manganese ions. The exchange splitting decreases nearly linear when the number of Mn3d electrons diminish – Fig.12 [21,22].

The magnetic circular dichroism (MCD) in the core level X-ray absorption spectroscopy (XAS) revealed also as a powerful method used to analyze the magnetic properties. The Ni2p→3d XAS-MCD spectra at 25 K, in $GdNi_2$, are plotted in Fig.13a [23]. The MCD spectrum was defined as I_+-I_- where I_+ and I_- denote the absorption intensities with the photon parallel and antiparallel to the direction of the magnetic field, respectively.

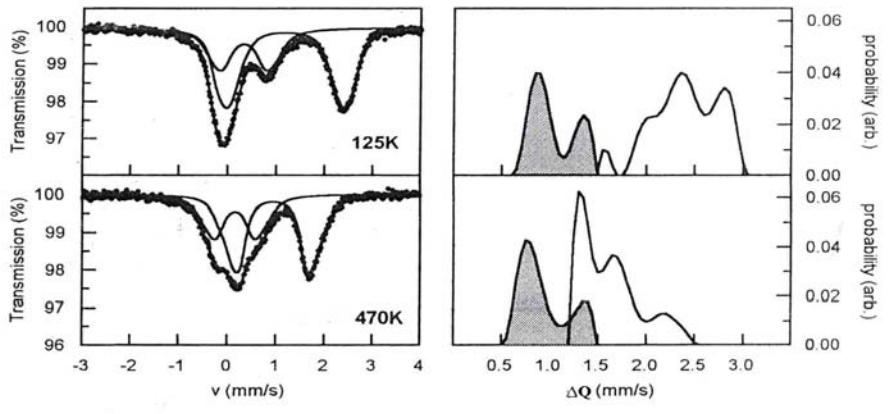

Fig. 10

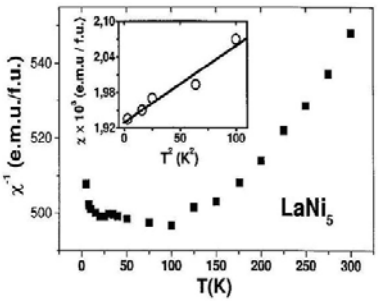

Fig. 11a

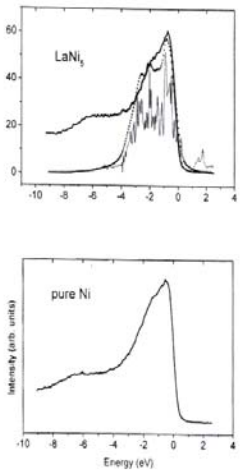

Fig. 11b

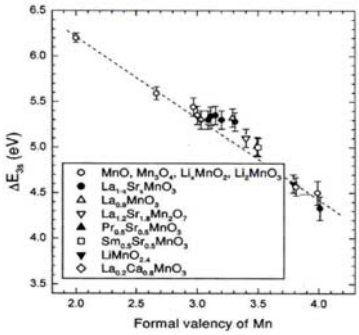

Fig. 12

The Ni2p→3d XAS spectrum consists of the L_3 and L_2 components split by spin-orbit interaction of the core hole. The L_3 region of the XAS spectrum has three peaks (A,B,C) qualitatively similar to those of pure Ni. The MCD spectrum in the L_3 region has also three peaks A', B', C' which correspond to A, B and C in XAS. The sign is positive in the L_3 region and negative in L_2 region. From the MCD spectrum, spin and orbital contributions of Ni, μ_L=0.06 μ_B and μ_S=0.14 μ_B, were obtained. For Gd3d→4f XAS-MCD spectrum, can be shown that the sign is negative in the M_5 region and positive in the M_4 region. This means that there is an antiferromagnetic coupling of Gd and Ni moments. By magnetic measurements on $GdNi_2$ a value of 7.00 μ_B/f.u. was obtained and thus Ni was supposed to be nonmagnetic. Band structure calculations show that the Gd moment is 7.29 μ_B (including 5d band polarization) antiparallel oriented to a nickel moment of ≅ 0.15 μ_B. This agree with the value obtained by magnetic measurements, the 5d band polarization being compensated by Ni moment.

The perturbed angular correlations method give also useful information, as for example, on the magnetic hyperfine interaction or concerning the defects in lattice. A series of PAC spectra of ^{111}Cd:$TbCo_2$ are plotted in Fig. 14 [24]. At 10 K the spectrum shows periodic modulation of the anisotropy, typical for a perturbation by a pure magnetic interaction with the precession amplitude decreasing only weakly with increasing time.

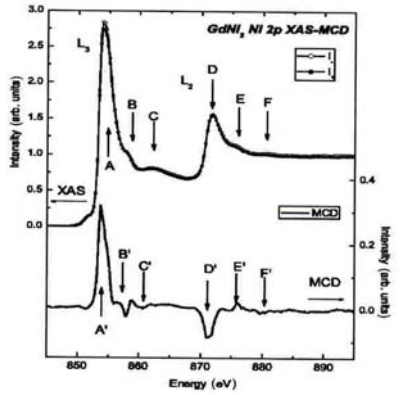

Fig. 13a

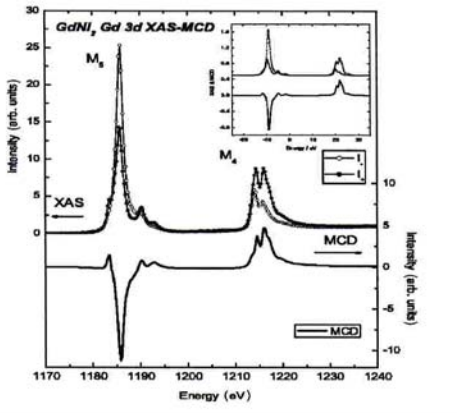

Fig. 13b

The precession frequency, ν_M, decreases with increasing temperature, but the attenuation of the oscillation amplitudes are not affected. At about $T/T_C \cong 0.97$, the attenuation starts to increase and within 2-3 K, the oscillations are completely wiped out. The PAC spectra change from the periodic modulation characteristic to ferrimagnetic phase to the constant anisotropy of the paramagnetic phase. At $T/T_C \geq 0.97$, two fractions of PAC probe are present. The paramagnetic fraction increases with temperature as showed in Fig. 15. The temperature dependences of the magnetic interaction frequencies, ν_M, of ^{111}Cd in compounds which show a second order transition are more close to the prediction of Stoner model that of the molecular field - Fig.16. For R = Dy, Ho, Er a first order type transition was shown.

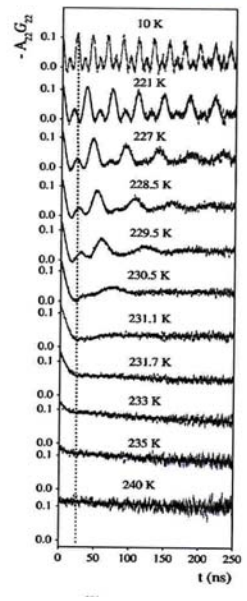

Fig. 14

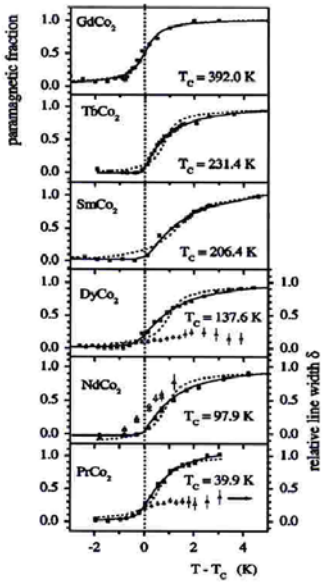

Fig. 15

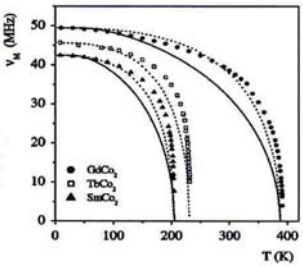

Fig. 16

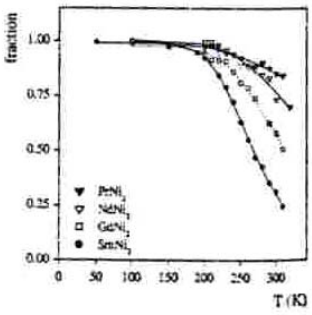

Fig. 17

Single phase $R_{1-x}Ni_2$ compounds can be obtained, in some cases only with rare-earth deficit. Values x=0.056 were obtained for R=Pr and x=0 for R=Lu. These compounds have a C15 superstructure (space group $F-\bar{4}3m$), in which 4a sites of R sublattice are partly occupied. The instability was attributed to r_R/r_{Ni} ratio much larger than that of the most compact C15 arrangement of hard spheres. Although ^{111}Cd resides on the cubic R site, a strong axially symmetric quadrupole interaction (QI) was observed for R=Pr, Nd, Sm, Gd. The fraction of probe nuclei subject to the QI decreases from 100 %, at low temperatures, to zero at T>300 K (R=Sm,Gd) or T>500K (R=Pr,Nd) – Fig. 17 [22]. The above feature can be explained by :(1) the mother isotope ^{111}In of the PAC probe ^{111}Cd constitutes an attractive potential for vacancies and (2) the R vacancies in $R_{1-x}Ni_2$ are highly mobile at T<300 K. The probe-vacancy binding energy decreases from light to heavy R constituents, which explain the absence of QI in heavy R compounds. At T>500 K nuclear spin relaxation, related to vacancy hopping, was observed in nearly all $R_{1-x}Ni_2$, also most of those that show no static QI at low temperatures.

The above examples show the broad spectra of information that can be obtained by analyzing a magnetic material by using different experimental methods. These will be reviewed, during the summer school. In addition to their physical bases, representative studies by using various experimental methods will be also presented by the well-known specialists in the field.

References

1. P.Weiss, J. Phys. 6, 667 (1997)
2. L.Néel, Ann. Phys. 3, 137 (1948)
3. E.Burzo, A.Chelkowski, H.R.Kirchamyr, Landolt Börnstein Handbuch, vol. 19d2, 1990, Springer Verlag
4. G.E.Fish, J.J.Rhyne, S.G.Sankar, W.E.Wallace, J. Appl. Phys. 50, 2003 (1979)
5. R.Lemaire, Cobalt 32, 132 (1966)
6. B.Decrop, J.Deportes, R.Lemaire, J. Less Common Met. 95, 1 (1983)
7. E.Zavoisky, J. Phys. USSR 9, 21 (1944)
8. J.H.E.Griffiths, Nature, 158,670 (1946)
9. E.Burzo: in New Frontiers in Rare-Earth Science and Applications vol. II, p. 948, Beijing, 1985
10. R.K.Vangsness, Am. J. Phys. 24, 60 (1956)
11. E.Burzo, I.Ursu, J. Appl. Phys. 50, 1471 (1979)
12. E.Burzo, Fizica Fenomenelor Magnetice, vol. III, Editura Academiei Romane, 1983
13. E.Burzo, R.Baican, in Proc. XVIII Congress AMPERE, North Holland 1976, p.151
14. F.Bloch, W.W.Hansen, M.Packard, Phys. Rev. 70, 474 (1946); E.M.Purcell, H.C.Torrey, R.V.Pound, Phys. Rev. 69, 37 (1946)
15. A.Oppelt, K.H.J. Buschow, Phys. Rev. B13, 4698 (1976)
16. Y.Yamada, H.Ohmae, J. Phys. Soc. Jpn. 48, 513 (1980)
17. R.L.Mössbauer, Z. Phys. 151, 124 (1958)
18. P.J.Viccaro et al, J. Appl. Phys. 50, 2051 (1979)
19. J. de Grave et al, Am. Mineral. 87, 132 (2002)
20. E.Burzo, S.G.Chiuzbaian, L.Chioncel, M.Neumann, J. Phys.: Condens. Matter 12, 5897 (2000)
21. V.R.Galathov et al, Phys. Rev. B 65 113102
22. M.Neumann et al, Mold. J. Phys. (in press)
23. M.Mizumaki et al, Phys. Rev. B 67, 132404 (2003)
24. M.Forker, S.Müller, P. de la Presa, A.F.Pasquevich, Phys. Rev. B 68 014409 (2003)
25. M.Forker et al, Phys. Rev. B 70, 014302 (2004)